

## EXPERIMENTAL INVESTIGATION OF IMBIBED OPEN-CELL FOAMS UNDER REPETITIVE COMPRESSION

Georgian-Cristian LUPU<sup>1</sup>, Aurelian FĂTU<sup>2</sup>, Yann HENRY<sup>3</sup>, Ionuț-Răzvan NECHITA<sup>4</sup>, Traian CICONE<sup>5</sup>

*An original experimental test bench was developed to investigate the behaviour of fully imbibed soft, porous materials under repetitive compression. When fluid is squeezed out of the porous structure, under compression, its resistance to flow develops a high load capacity. This mechanism, specific to ex-poro-hydrodynamic lubrication (XPHD), depends on permeability variation with porosity.*

*The influence of porosity, initial compression, and compression amplitude were investigated on two open-cell foams, subjected to several compression sequences with different frequencies. Preliminary results obtained with oil show that the capacity of open-cell foams to reabsorb the fluid during the return stroke reduces with the frequency, influencing the maximum pressure generated inside the porous matrix and limiting the potential benefits of the XPHD lubrication film.*

**Keywords:** oscillating squeeze, open-cell foams, soft, porous.

### 1. Introduction

Porous layers have long been considered an attractive alternative for impermeable surfaces in squeeze film lubricating mechanisms typically encountered in applications like rotating bearings, dampers, wet clutches, or synovial joints [1]. Using porous materials in squeeze film lubrication offers some advantages, like the ability to correct surface misalignments, or to reduce heat. These materials also show reduced sensitivity to contaminants present in lubricants.

These applications involve the cyclic alternance of positive and negative loads during operation. The approach of two opposing surfaces causes an increase in fluid film pressure, referred as positive squeeze effect. Conversely, when these surfaces move apart, the fluid is reabsorbed into the gap between them, causing a

<sup>1</sup> Researcher, Eng., Military Equipment and Technologies Research Agency, Romania, e-mail: glupu@acttm.ro

<sup>2</sup> Prof., Département Génie Mécanique et Systèmes Complexes, Institut PPRIME, CNRS – Université de Poitiers – ENSMA, UPR 3346, France, e-mail : aurelian.fatu@univ-poitiers.fr

<sup>3</sup> Assoc. prof., Département Génie Mécanique et Systèmes Complexes, Institut PPRIME, CNRS – Université de Poitiers – ENSMA, UPR 3346, France, e-mail : yann.henry@univ-poitiers.fr

<sup>4</sup> PhD student, Machine Elements and Tribology Department - University POLITEHNICA of Bucharest, Romania, e-mail: ionut\_razvan.nechita@upb.ro

<sup>5</sup> Prof., Machine Elements and Tribology Department - University POLITEHNICA of Bucharest, Romania, e-mail: traian.cicone@upb.ro

negative squeeze. Under specific conditions, cavitation may occur within the fluid film during the negative phase. The study of cavitation in deformable porous media [2] or in oscillating porous squeeze films [1] has been of interest in recent papers, indicating that it is still a complex topic that needs further investigation.

When soft, porous materials are fully imbibed and subjected to compression, the fluid squeezing out of the pores leads to a different type of lubrication, also known as to ex-poro-hydrodynamic lubrication (XPHD [3]). The porosity of the solid matrix varies with compression, modifying the permeability of the medium generating thus load capacity. The contribution of the solid matrix to load support is neglected. This lubricating mechanism has been extensively investigated ([4], [5], or [6]) showing a good potential for impact attenuation in one-time use applications, such as protection helmets, or in thrust bearings. The results obtained by *S. Kunik* in [7] have also proved the usefulness of the XPHD mechanism for applications that use fluid dislocation during sliding motion, functioning in repetitive compression strokes.

A significant amount of literature can be found on the subject of oscillatory squeeze film in bearings, specifically when using a porous rubber material. In their study [8], *Kaneko et al.* concluded that the high frequency sinusoidal movement between two bearing surfaces, when one is made of a deformable and permeable medium, is affected by the material's viscoelasticity and fluid inertia force. These factors should be considered when assessing the lubrication characteristics of the bearings. Other papers ([9], [10]) focus on the influence of surface roughness and permeability of the porous material on the hydrodynamic force generated in the squeeze film between a rigid surface and the rubber. However, it is important to note that the oscillatory squeeze film between two surfaces, when using a porous rubber, falls under the domain of elastohydrodynamic lubrication, as the flow is influenced more by the elastic deformation of the rubber, than by its porosity.

When it comes to repetitive compression of fully saturated porous materials the literature available is scarce, indicating the need for further research to understand fluid flow in these situations. As part of this effort, an experimental test bench was developed to study how the compression frequency affects the behaviour of porous materials. The impact of porosity, initial compression, and compression amplitude were investigated. The repeatability of the results was also checked by subjecting the samples to several compression sequences with various frequencies.

This paper introduces the novel testing device and reports the findings from preliminary experimental campaigns. The experiments involved testing open-cell foams imbibed with oil. The results show that the ability of porous materials to re-imbibe, during the return phase, represents an essential condition for repetitive compression.

## 2. Experimental test bench, materials, and working procedure

The experiments presented in this paper have been performed on a new, specially designed test bench (fig. 1a) with the following specifications:

- symmetrical compression-return strokes with linear periodic pattern;
- the relative position of the compression surfaces can be adjusted to assess materials with different thicknesses or to apply an initial compression level;
- compression frequency is variable in the range 0.5÷12 Hz;
- force and displacement are measured over time.

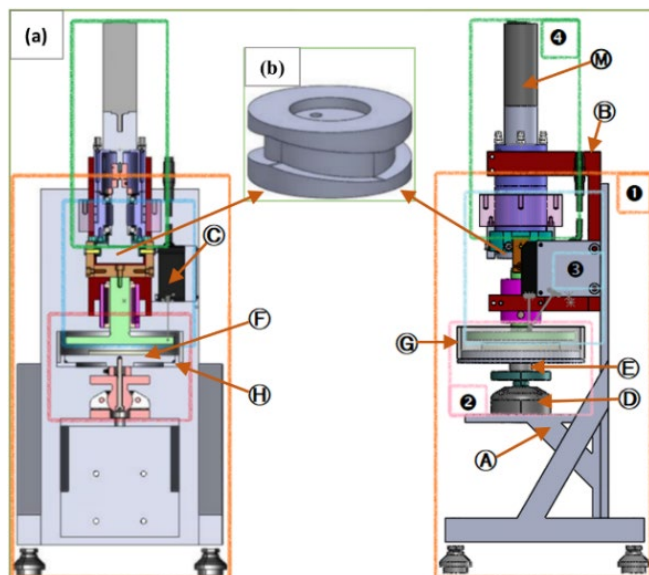


Fig. 1. Experimental device: (a) Front section and side view (b) Cylindrical grooved cam

The main parts of the test rig are the rigid frame ①, the fixed plate ②, the compression plate ③ and the motor ④. The central element of this device is a cylindrical grooved cam (fig. 1b), which is fabricated in two versions: one with a compression amplitude of 2.2 mm and the other with 4.5 mm. Its role is to convert the rotation of the driving shaft into reciprocating motion to actuate the compression plate. To achieve higher compression frequencies, the cam has symmetrical profiles that generate two complete strokes for each rotation.

On the rigid frame ①, an L-shaped support ⑦ sustains the fixed plate assembly. Another part, but U-shaped ⑧, firmly locates the motor assembly and holds the displacement sensor ⑥. The position of the two supports can be adjusted vertically, to set different distances between the compressing surfaces.

The fixed plate assembly ② is joined to the L-shaped part through a ball joint mounting flange ⑨. This component is used to align the compressing surfaces and also has a central groove that allows the pre-tensioning of the axial force

transducer **E** between the flange and the fixed plate **F**. A transparent tube **G**, which allows the visualisation, is mounted on a holder frame **H** to form a fluid reservoir, around the edge of the fixed plate. The experimental cell is sealed to prevent fluid leakage.

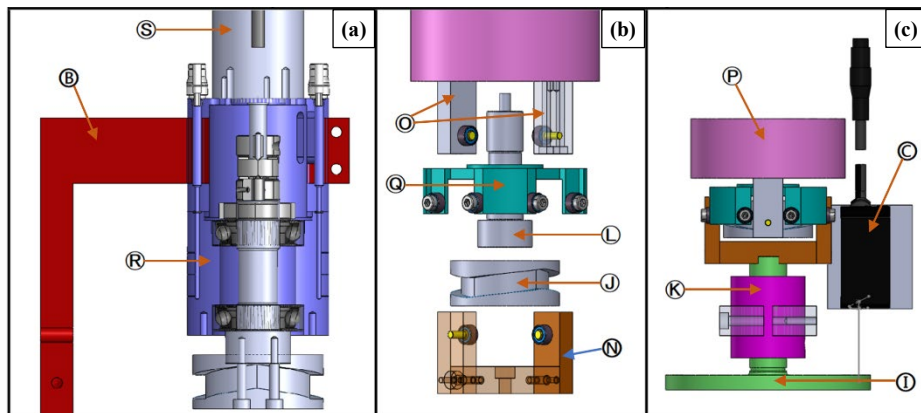


Fig. 2. (a) Motor assembly section (b) Rotation-to-translation assembly (c) Upper plate assembly

The compressing plate assembly ❸ (fig. 2b and 2c) includes the upper plate ❶, the grooved cam ❷, the displacement sensor, and the parts that ensure the driving and balancing of the plate. The compression plate is guided by an aerostatic bearing ❹. The cam is mounted at the end of a shaft ❻ coupled to the electric motor ❻. Two ball bearings mounted on a U-shaped part ❻ push the plate, channelled by the profiled groove. At the same time, another pair of bearings mounted on extension rods ❻, move the counterweight ❻ in the opposite direction, to balance the weight of the plate. The axes of the two pairs of bearings are perpendicular to each other. To sustain the translational movement, the U-shaped part and the rods are sliding between four sets of ball bearings mounted on a rotation locking part ❻. This part is connected to the bearing case ❻ of the shaft located in the motor assembly.

In the motor assembly ④ (fig. 2a) a variable speed VDC motor drives the cam shaft through a planetary gear ⑤. For the 3000 rpm of the motor, the gearset assures a constant torque of 3Nm. The shaft casing has four air channels that ensure the counterweight is sliding without friction on its exterior surface.

**Instrumentation.** Axial force is measured using a Kistler 9031A piezoelectric transducer and a Kistler 5015A charge amplifier. As the forces developed were less than 1 kN, the transducer was used only in its first calibrated range ( $\pm 6$  kN or 10%), where it has a very good linearity.

The displacement of the upper plate is acquired with a Keyence LK-050 optical sensor using a 20 Hz acquisition frequency. The sensor communicates with a computer through an NI 9215 acquisition card.

The temperature of the fluid is measured using a thermocouple fixed as close as possible to the foam's outer radius. During all the experiments, the temperature of the fluid rarely changed by more than 1.5°C, usually influenced by the ambient temperature when the duration of some tests was long. Therefore, the fluid viscosity variation was neglected.

**Materials.** Specimens having 60 mm in diameter were cut using laser technology from two types of polyurethane foams. Commercially known as Collar®2404 and Collar®2406, these foams have been thoroughly investigated by Kunik [7] during his PhD studies, carried at Institute Pprime (University of Poitiers, France). The properties of the foams are presented in table 1. These materials will be referred as F2404, respectively F2406. The fluid used in these experiments, a MA4 FE 5W30 engine oil, has a viscosity of 0.105 Pa · s at 23°C.

Table 1

Properties of polyurethane foams used in experiments ([11], [7])

Property	Unit	Collar® 2404	Collar® 2406
Thickness	mm	10	
Bulk density (DIN 53420)	kg/ m <sup>3</sup>	40	36 ÷ 39
Compression resistance (at 40%)	kPa	4.5	5.3 ÷ 6.3
Porosity (microtomography, precision 5.74 µm) [7]	—	0.960	0.970
Mean pore diameter	mm	0.667	0.549

A **working procedure** was defined in order to assess the compression of samples in a dry state (as a reference) and then, imbibed with fluid, using both cams.

The steps of the working procedure are as follows:

- initial set-up of the maximum gap (fig. 3a): with the moving plate in the uppermost position of the grooved cam (fig. 3b, left), the maximum distance ( $h_{max}$ ) between the compression surfaces is set by moving the fixed plate assembly;
- surface parallelism between the two plates is checked;
- displacement reference is initialised ( $y_p = 0$ ) in LabView;
- the sample is placed and glued on the fixed plate;
- the sample is imbibed with a small quantity of fluid and manual compression-return strokes are performed to take out the air;
- force reference is initialised in LabView;
- the holder frame is fixed on the plate and 150 ml of fluid are poured in;
- the voltage of the power supply is set to actuate the upper plate at an imposed frequency.

The first strokes are performed at low frequency to completely evacuate the air and ensure the foam full imbibition. Then, frequency is varied according to the test objectives. After each change, an “operational” pause is taken to allow the fluid to stabilise and the material to adapt to the new stress level.

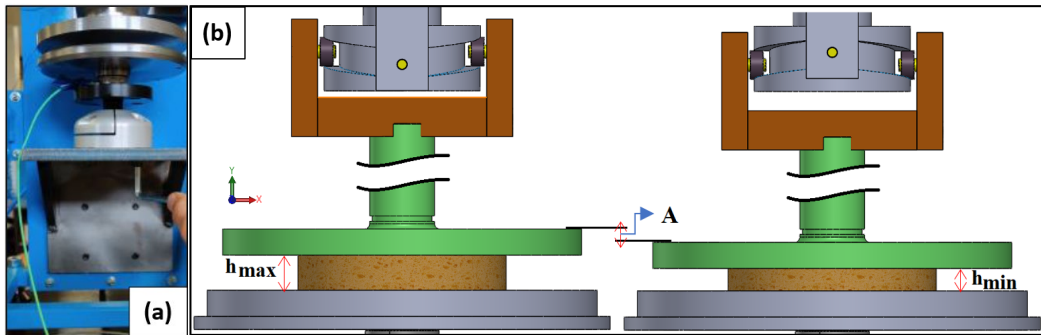


Fig. 3. (a) Initial set-up (b) Uppermost (left) and lowermost (right) positions of the moving plate

Afterwards, force and displacement variations are continuously acquired for at least five second, to ensure minimum 4÷5 complete strokes. Different configurations were used to evaluate the impact of porosity, initial compression, and compression amplitude on the samples. The repeatability of the results for each configuration was assessed by repeating the same test procedure several times.

### 3. Experimental data analysis

The processing of the experimental raw data is briefly explained in the following.

**Compression frequency** should be influenced only by voltage. But, as some disturbing factors cannot be entirely eliminated (e.g., friction, wear, etc.), this parameter exhibits small fluctuations over the acquisition interval, especially at lower values. In consequence, mean frequency ( $\bar{f}$ ) is used when representing experimental data in the graphs:

$$\bar{f} = \frac{1}{n} \sum_n \frac{1}{T_n} \quad (1)$$

where  $T$  is the time interval between two consecutive maximum (or minimum) points and  $n$  is the number of intervals used for the calculation.

**Porosity** of the foams varies during experiments and depends on the sample thickness (i.e., compression level). The maximum porosity ( $\varepsilon_{max}$ ) and the minimum porosity ( $\varepsilon_{min}$ ) indicate the porosity in the uppermost and the lowermost positions during compression. Their values are calculated from the initial compression of the material ( $c_0$ ) and the amplitude ( $A$ ) of the grooved cam, using the assumptions of solid fraction conservation and constant transverse area [6]:

$$h_0(1 - \varepsilon_0) = h(1 - \varepsilon) = const. \quad (2)$$

where  $h_0$  is the initial thickness,  $\varepsilon_0$  the initial porosity and  $h$  and  $\varepsilon$  represent the thickness and porosity of the compressed material. The micro-computed tomography ( $\mu$ CT) value from table 1 is used for  $\varepsilon_0$ . The extreme values of the sample thickness are:

$$h_{max} = h_0 - c_0 \quad (3)$$

$$h_{min} = h_0 - c_0 - A \quad (4)$$

**Force.** In the case shown in fig. 4, the horizontal scale is set to cross the displacement scale at 3.5 mm below  $h_0$ . This is done to mark  $c_0$  and the uppermost position of the moving plate ( $h_{max}$ ). The “0” value on the left vertical scale marks the initial thickness of the material.

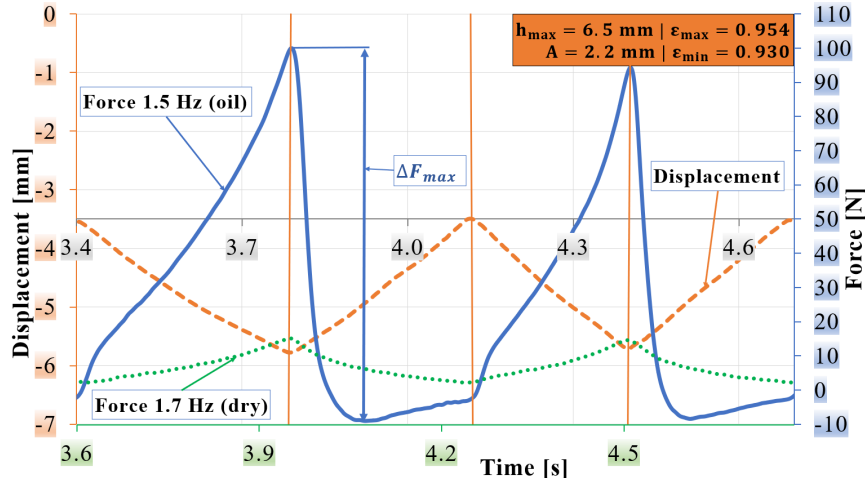


Fig. 4. Type of experimental data acquired (F2406)

From fig. 4, it can be observed that the force reaches its maximum value at the end of the compression stroke, as it is expected, whilst the minimum negative value is attained after a fraction of the return stroke. The moment of negative force occurrence depends on the compression frequency. In the case of the dry specimen, the zero-point error of the piezoelectric sensor was not considered. However, this is not an important issue because this graph is intended to show the difference between the dry and imbibed state of the foam.

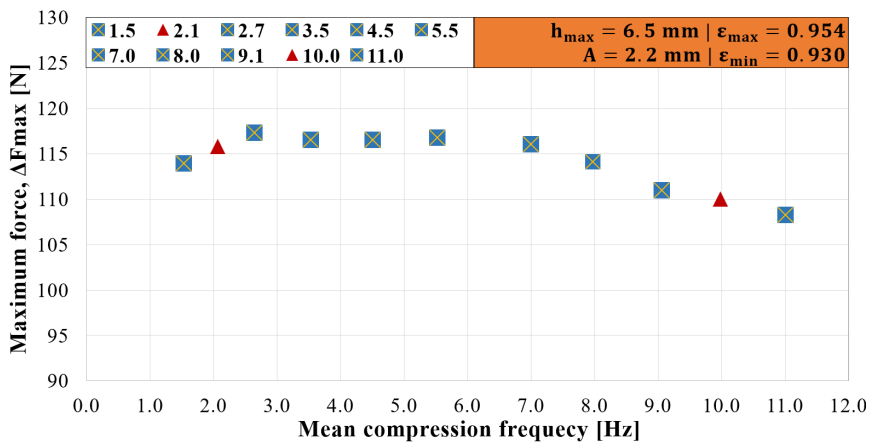


Fig. 5. Maximum force variation with compression frequency (F2406)

When comparing the dry and imbibed tests of the same specimen, it can be observed that there are some significant differences, especially on the return stroke. While for the dry specimen the shape of the force profile is almost mirrored for the compression-return strokes, the return stroke of the imbibed foam differs a lot in shape. This behaviour is attributed to the material which starts to get re-imbibed, generating a suction force that is opposing resistance to the plate's displacement. This also explains the negative forces recorded during this stage.

**Maximum force (pressure).** During experiments, both positive and negative values are obtained for the force. Therefore, force is expressed based on the maximum absolute value recorded at a specific frequency, throughout the entire acquisition interval. The reaction of the material to compression acquired as normal force is further calculated and used in terms of normal pressure.

The maximum value identified for each frequency is used to build graphs similar to the one depicted in fig. 5. This graph shows that, up to approximately 3Hz the maximum force increases linearly and between 3÷6 Hz the parameter remains constant. For higher frequencies, the force decreases linearly. This behaviour was observed throughout all the experiments, with differences in terms of the frequency at which the extreme values appeared.

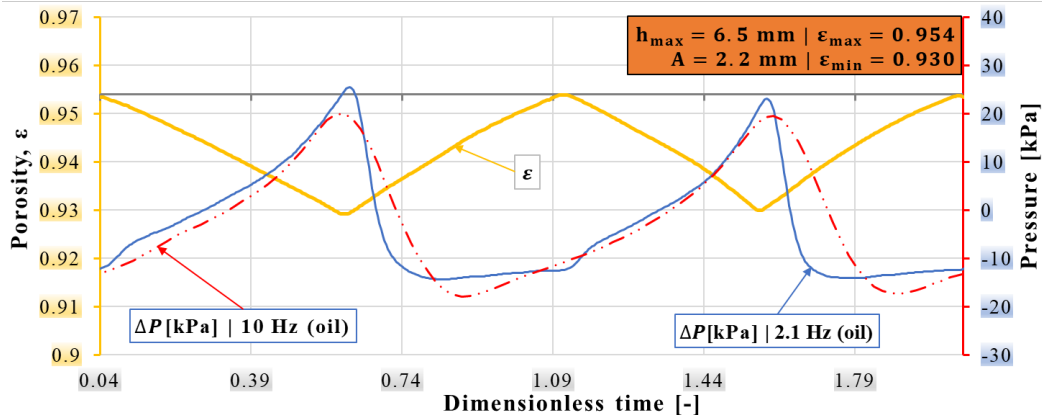


Fig. 6. Calculated pressure and porosity (F2406)

To compare tests made at different frequencies, dimensionless time ( $\bar{t}$ ) is used and it represents the number of strokes:

$$\bar{t} = t \cdot \bar{f} \quad (5)$$

where  $t$  is the duration of the experiment. Fig. 6 shows the calculated pressure and porosity for the two points marked with triangles on the curve from fig. 5. Porosity is calculated from the displacement profile, using equation (2), and when using  $\bar{t}$  only one profile is represented for both frequencies.

In terms of pressure variation, for the two frequencies analysed in fig. 6, it can be observed that the curve shape at higher frequency is smoother than at lower frequency. Also, the local maximum and minimum turning points have different

slopes. Whilst at lower frequency pressure profile is sharper at the end of the compression phase and flattened to the end of the return stroke phase, at higher frequency the pressure has similar shapes on both phases. The discontinuity appearing during the return stroke at lower frequencies vanishes and the curve becomes smoother.

This can be explained by the fact that, at higher frequencies, the rate of fluid reabsorption cannot keep the pace with the plate movement, and the cavitation has not enough time to develop. Also, as a consequence, at the end of the return stroke the material is not completely imbibed. Because a new compression stroke starts with the material partially filled with fluid, lower values for  $\Delta P_{max}$  are recorded.

#### 4. Results and discussions

In the following part, the influence of different parameters on the maximum pressure variation will be analysed. In the case of dry samples assessed, the results do not vary too much with frequency. For F2404, the maximum pressure varies in the range 5.1-5.7 kPa, while for F2406, it fluctuates in the range 5.2-6.2 kPa.

**Porosity effect.** Porosity influences both fluid expulsion and reabsorption in the porous material.

The results obtained for the two foams can be analysed from fig. 7 where third order polynomial curves were fitted. To facilitate the comparison with the dry tests, maximum pressure is set to start from 5kPa.

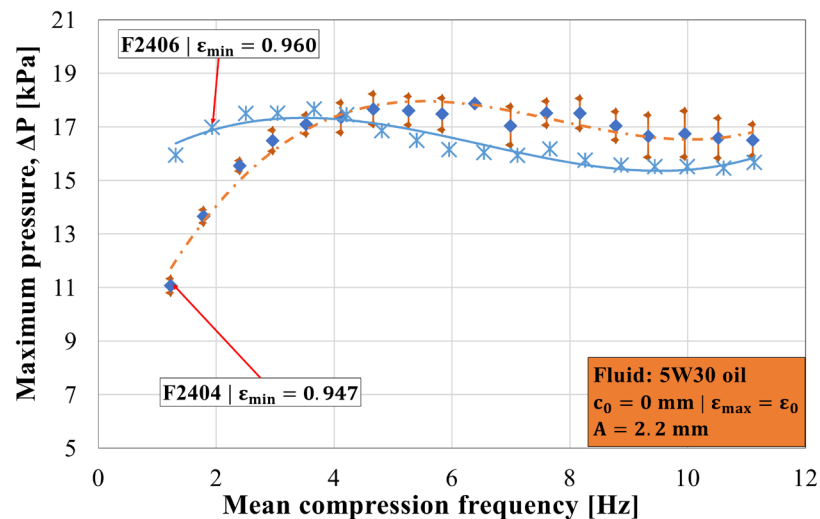


Fig. 7. Maximum pressure variation with mean frequency – different porosities

For F2404, three consecutive test routines are represented in the form of averaged values with standard deviation. The average standard deviation for maximum pressure is less than 0.5 kPa with a maximum of 0.85 kPa. This can be interpreted as: maximum pressure decreased with 1 kPa on average between first

and third test routine. The duration of the first test was 40 min, 35 min for the second one while for the last test, 25 min were needed to obtain the eighteen points.

When analysing the result from one test made on F2406 sample, in the same conditions, one can observe that the profile of maximum pressure variation with frequency is similar to the one obtained for F2404, but with a shift to the left for the frequency at which the highest value is recorded. This behaviour can be explained by the fact that F2406 solid matrix is more resistant to compression, as seen from the values given in table 1.

The maximum pressure, for the two foams, when compared to the dry results, is 2÷3 times higher. The foams show the tendency to oppose less resistance with the increased number of tests performed in time and with frequency, as the reimpbibition capacity of the material diminishes. The pressure increase between the dry and imbibed conditions is due to the fluid contribution on both squeeze phases.

As the maximum strain level of the foams during the tests presented (0.22) is less than the densification strain (typically above 0.6 for polyurethane foams) but above linear elastic region (typically less than 0.1) the samples compression is in the plateau strain regime, as defined by *Gibson and Ashby* in [12]. According to *Dawson et al.* [13], in this region, an open-cell foam imbibed with a Newtonian fluid subjected to dynamic compression (specific to impact applications) behaves in a bimodal regime: a linear-elastic regime and a densified one. The densified regime is assumed to be initiated in the middle of the foam and to be bounded by two elastic regions: one stationary (below the densified region) and one moving with the upper plate (above) [13]. These observations could also provide an explanation for the behaviour of the analysed foams.

The difference in porosities (F2404 has the smaller value) combined with the mean pore diameter (F2406 has the smaller value) could influence the “thickness” of the densified region. This could explain the difference in maximum pressures between the two materials at low frequencies. The lower pore size of F2406 favorizes imbibition and the ability of the foam to transport fluid, increasing its resistance to the fluid flow at lower frequencies. At higher frequencies, when the foams fail to get fully imbibed, they start to behave in an equivalent way. The viscosity of the fluid impacts additionally the ability of the foam to reabsorb, during the return stroke, the entire volume of the fluid expelled during compression.

**The influence of the compression amplitude.** Fig. 8 (a) shows the results of two tests done on F2404 samples with different amplitudes but the same minimum thickness (the same  $\varepsilon_{min}$ ). As a consequence, the shapes of the maximum pressure-frequency curves are similar. However, in the tests done with the 4.5 mm cam, maximum pressure values are 6÷8 times higher than those obtained for dry samples, while for the 2.5 mm initially compressed foams and 2.2 mm cam, maximum pressures are only 4÷5 times higher. The higher pressures obtained with the 4.5 mm cam can be explained by the fact that, in the lower part of the foam,

more pores remain blocked with fluid, increasing flow resistance. Also, the plate travels more which provides more time for the material to reabsorb the fluid. The densification regions [13] for the two configurations are different also, leading to a reduced active elastic region for the initially compressed foam and thus resulting into a softer response.

For F2406, results above 7.5 Hz with the 4.5 mm cam could not be obtained, as can be seen from fig. 8 (b). This was due to a loss of fluid volume, as droplets of oil started to be expelled out from the reservoir. Only one curve was obtained with the same quantity of fluid as for F2404 and was used in the comparison.

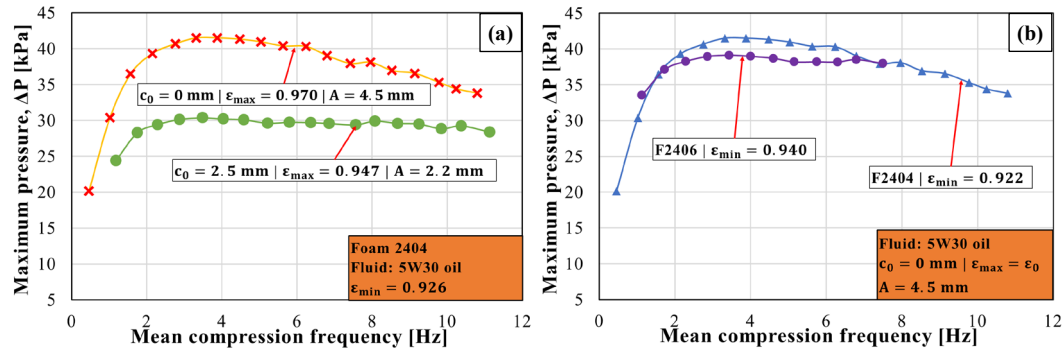


Fig. 8 Maximum pressure variation with mean frequency – different compression amplitudes:  
(a) F2404 (b) F2404 vs. F2406

The maximum pressures obtained for the two types of foams have the same order of magnitude. Compared to the dry samples, maximum pressure of the imbibed F2406 sample is 6 times higher. The higher values in maximum pressures for F2404 could be explained by a more reduced value for porosity at the end of the compression stroke. A material with lower porosity allows less fluid to be expelled from the foam which leads to a pressure increase in the imbibed material.

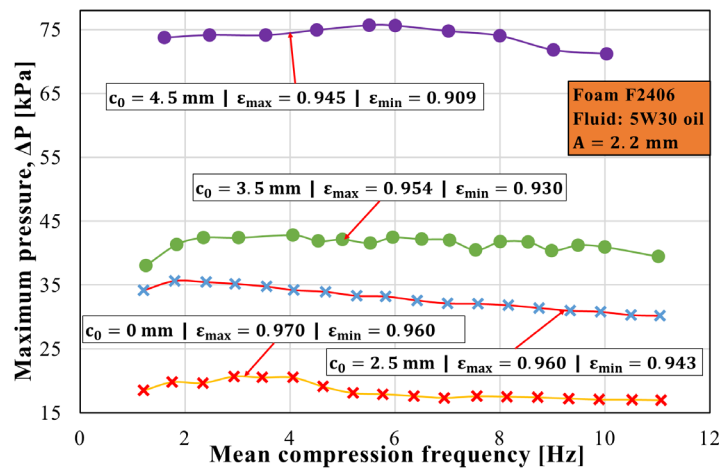


Fig. 9 Maximum pressure variation with mean frequency – different initial compression

**The influence of the initial compression.** With the 2.2 mm grooved cam, two additional values were investigated for  $c_0$ . When  $c_0 = 3.5 \text{ mm}$ , the samples are compressed between  $h_{\max} = 6.5 \text{ mm}$  and  $h_{\min} = 4.3 \text{ mm}$ . For  $c_0 = 4.5 \text{ mm}$ , the thickness of the foams varies between  $h_{\max} = 5.5 \text{ mm}$  and  $h_{\min} = 3.3 \text{ mm}$ .

Fig. 9 shows that, when  $c_0$  is 0, 2.5 or 3.5 mm, the maximum pressure-frequency curves increase gradually as porosity reached in the lowermost position is more reduced. For the smallest thickness reached during testing (3.3 mm) the results are almost double than the nearest one, that is with only 1 mm higher at the end of compression.

An explanation for this behaviour may come also from the compression stages defined by *Gibson and Ashby* in [12]. When the sample reaches 3.3 mm thickness at the end of compression, the material might be close to its junction point between plateau and densification stage or already in densification region.

**Results repeatability.** Fig. 10 depicts the results obtained with the two samples in tests made with very close values of the extreme porosities in a compression cycle. The graphs show the values from five different tests performed on the same F2406 sample and nine tests performed on an F2406 sample, respectively.

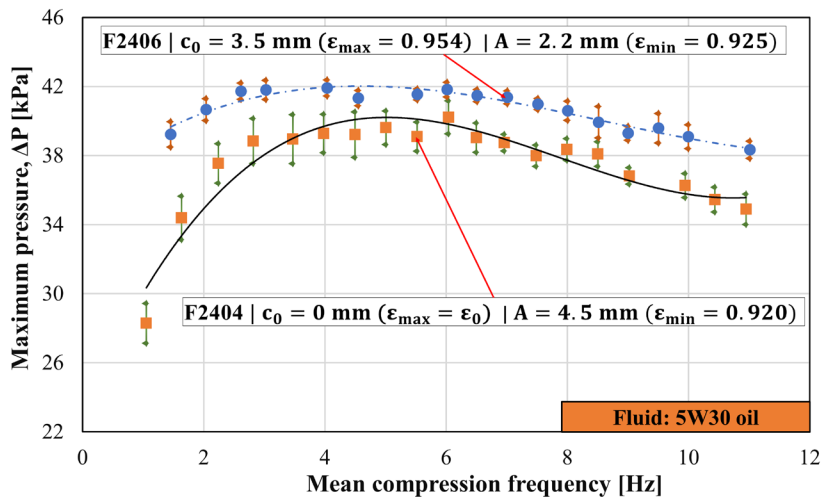


Fig. 10 Maximum pressure variation with mean frequency – repeatability

The mean value of the standard deviation of all points obtained for F2404 is less than 1 kPa and the maximum value is around 1.45 kPa. This is less than 5% of the minimum pressure difference. We can affirm that, despite the reduction of maximum pressure between consecutive testing routines, the material shows a good repeatability of the tests performed in the same configuration. Except for some critical frequencies (like 6 or 8.5 Hz) the behaviour of F2404 seems to be the same, for every  $c_0$  and  $A$  evaluated.

The averaged standard deviation for the tests performed on the same F2406 sample is less than 0.55 kPa with a maximum value of 0.9 kPa. The observations made for F2404 foam are valid also for the F2406 foam. Some critical frequencies can also be seen in these curves (like 4.5 and 5.5 Hz), but the spread of the results is better than in the other case.

The behaviour of these foams, after 3÷4 Hz, is influenced by the insufficient reabsorption of fluid and could also be limited by air intake during the return stroke. When air occupies some of the pores, this leads to reduced pressure values.

One can also remark that the maximum pressures show a similar evolution, in the same range, which supports the idea that porosity influences especially the frequency at which we obtain the highest maximum pressure.

## 5. Conclusions

An original experimental test device was built to investigate soft, porous materials imbibed with fluids and subjected to repetitive compression strokes. The preliminary results obtained show that the capacity of the material to reabsorb the fluid during the return stroke reduces with the frequency.

The foam samples presented herein were subjected to several compression-return strokes and the results for the same testing configuration are similar, with minor differences in some “critical” frequencies. As these are preliminary experiments, the spread of the results can be considered good. The difference in maximum pressure for the same frequencies can be caused by a series of factors as manufacturing tolerances and faults, resonance frequency of some components or misalignment of the compression surfaces and thus will need further investigations.

The experimental evidence show that porosity impacts especially the frequency at which the highest maximum pressure is obtained. A material with lower porosity tends to reach its highest difference in pressure at a greater frequency.

Low compression frequencies create favourable conditions for the material to be completely imbibed with fluid at the end of the return stroke.

Maximum pressure variation with frequency depends on initial compression and compression amplitude. Lower the thickness, a more rigid response of the imbibed foams is observed, as the solid matrix contribution to pressure build-up increases. The rigid behaviour is also caused by the reduction of porosity (and thus permeability) with compression, as more pores remain blocked with a small amount of fluid inside, being unable to fully expulse it. These observations are in line with previous results obtained when trying to characterise a limit porosity (percolation threshold) of highly compressible foams in the densification zone [14].

### Acknowledgement

This work has been funded by the European Social Fund from the Sectorial Operational Programme Human Capital 2014-2020, through the Financial Agreement with the title “Training of PhD students and postdoctoral researchers in order to acquire applied research skills – SMART”, Contract no.13530/16.06.2022-SMIS CODE: 153734.

### R E F E R E N C E S

- [1] *S. Sobhi, M. Nabhani, K. Zarbane, M. El Khelifi*, “Cavitation in oscillatory porous squeeze film: a numerical approach”, in *Industrial Lubrication and Tribology*, vol. 74, no. 6, 2022, p. 636–644.
- [2] *Y. Leng, P. Vlachos, R. Juanes, H. Gomez*, “Cavitation in a soft porous material”, in *PNAS Nexus*, vol. 1, no. 4, 2022, p.150.
- [3] *M. D. Pascovici*, “Lubrication by dislocation: a new mechanism for load carrying capacity”, in *Proceedings of 2nd World Tribology Congress*, Vienna, 2001.
- [4] *T. Cicone, M. D. Pascovici, C. Melciu, P. Turtoi*, “Optimal porosity for impact squeeze of soft layers imbibed with liquids”, in *Tribology International*, vol. 138, 2019, p. 140–149.
- [5] *S. Kunik, A. Fatu, J. Bouyer, P. Doumalin*, “Experimental and numerical study of self-sustaining fluid films generated in highly compressible porous layers imbibed with liquids”, in *Tribology International*, vol. 151, 2020, p. 106435.
- [6] *M. D. Pascovici, T. Cicone*, “Squeeze-film of unconformal, compliant and layered contacts”, in *Tribology International*, vol. 36, no. 11, 2003, p. 791–799.
- [7] *S. Kunik*, Étude numérique et expérimentale du mécanisme de lubrification Ex-Poro-HydroDynamique (XPHD), PhD Thesis, Université de Poitiers, 2018.
- [8] *S. Kaneko, T. Tanaka, S. Abe, T. Ishikawa*, “A Study on Squeeze Films Between Porous Rubber Surface and Rigid Surface: Analysis Based on the Viscoelastic Continuum Model”, in *Journal of Tribology*, vol. 126, no. 4, 2004, p. 719–727.
- [9] *M. Mahbubur Razzaque, M. Mustafa*, “Effects of permeability and surface roughness on the behavior of an oscillating viscoelastic squeeze film”, in *Industrial Lubrication and Tribology*, vol. 65, no. 1, 2013, p. 37–43.
- [10] *M. Mustafa, N. J. Chhanda, M. Mahbubur Razzaque*, “A numerical model of an oscillating squeeze film between a rubber surface and a rigid surface”, in *Tribology International*, vol. 43, no. 1–2, 2010, p. 202–209.
- [11] \*\*\* <https://www.dimer.com/en/materialien/pur-weichschaum/pur-schaum.php>.
- [12] *L. J. Gibson, M. F. Ashby*, *Cellular solids. Structure and properties*, Ed. Cambridge University Press, 1999.
- [13] *M. A. Dawson, G. H McKinley, L. J. Gibson*, “The dynamic compressive response of open-cell foam impregnated with a Newtonian fluid”, in *Journal of Applied Mechanics*, vol. 75, no. 4, 2008, p. 041015.
- [14] *P. Turtoi, G. Lupu, T. Cicone, D. Apostol*, “Experimental investigation of the limits of fluid squeeze out from an imbibed porous material”, in *IOP Conference Series: Materials Science and Engineering*, vol. 997, no. 1, 2020, p. 012019.